On Numerical Simulation of Transition to Turbulence in Turbine Cascade

Petr Louda, Karel Kozel, and Jaromír Příhoda

Abstract The work deals with numerical simulation of transonic turbulent flow in turbine cascades taking into account transition to turbulence. The Favre-averaged Navier-Stokes equations are closed by the SST eddy-viscosity turbulence model or by explicit algebraic Reynolds stress turbulence model (EARSM) with the γ-ζ transition model of Lodefier and Dick. The mathematical model is solved by implicit AUSM-type finite volume method. The implementation of transition model does not require case specific input under the assumption that the whole thickness of boundary layer is contained in the same block of multi-block grid, which can easily be fulfilled in the cases considered. The results are shown for 2D tip profile turbine cascade and 2D and 3D SE1050 turbine cascade.

1 Introduction

The mathematical modeling of turbulent flow in turbine cascades serves as design tool as well as improves the understanding of complicated flow patterns typical of these flows. Mathematical models based on the Favre-averaged Navier-Stokes equations present acceptable accuracy at acceptable computational cost, however, the accuracy is influenced by turbulence model and its capability to predict bypass transition to turbulence. Correct prediction of turbulent boundary layer is important for heat exchange between blade and fluid and also can influence the losses e.g. by interaction with shock waves which is different on laminar boundary layer. Common two-equation eddy-viscosity turbulence models usually predict too early start of transition and then the transition is too fast. This problem is further emphasized by over-prediction of the turbulent energy production on the leading edge of the blade which has its origin in the eddy-viscosity assumption. Some ad hoc remedies of the

P. Louda (✉) • K. Kozel
Czech Technical University in Prague, Karlovo nám. 13, Praha 2, Czech Republic
e-mail: petr.louda@fs.cvut.cz; karel.kozel@fs.cvut.cz

J. Příhoda
Institute of Thermomechanics AS CR v.v.i., Dolejškova 5, Praha 8, Czech Republic
e-mail: prihoda@it.cas.cz

later problem has been proposed e.g. by Kato, Launder [3] or Medic, Durbin [10]. Better option is the use of more elaborate constitutive relation for turbulent stress as is the explicit algebraic Reynolds stress model (EARSM), e.g. the variant by Wallin [13] which is also used in this work. However the transition still requires explicit triggering. Considering transition models based on transport equations which seem more general than algebraic ones, the models contain equation for an intermittency variable and also for other auxiliary variable or variables. More recent examples are 3-equation model by Walters and Cokljat [14] or 2-equation model by Menter, Langtry [6]. Also 1-equation model is proposed by Durbin [1]. These models have "local" form enabling easy implementation especially on parallel computers. However they also share disadvantage of containing transition criteria implicitly. Any non anticipated mechanism of transition requires re-calibration of the model. In this work we apply the γ-ζ model of Lodefier, Dick [7] and Kubacki et al [5] instead. The model contains transition criteria explicitly and any new criterion can be added easily. The downside is that the model distinguishes free-stream and boundary layer and thus is not local. Nevertheless we show for typical 3D cascade geometry that when using multi-block grids the model is block-local and does not require case-specific input under assumption that the whole thickness of boundary layer is contained in one block, at least in region where transition occurs. This can be easily achieved with suitable O-type grid around the blade.

2 Mathematical Model and Numerical Method

2.1 Mathematical Model

The mathematical model of turbulent flow is based on Favre-averaged Navier-Stokes (NS) equations, see e.g. Wilcox [15]. The system consisting of continuity, 3 momentum and energy equations can be written in 3D in Cartesian coordinates as

$$\int_V \frac{\partial W}{\partial t} + \oint_{\partial V} F^I d\mathscr{S} = \oint_{\partial V} F^V dS, \tag{1}$$

$$W = \begin{bmatrix} \rho \\ \rho u_1 \\ \rho u_2 \\ \rho u_3 \\ \rho E \end{bmatrix}, \quad F^I = u_c \begin{bmatrix} \rho \\ \rho u_1 \\ \rho u_2 \\ \rho u_3 \\ \rho H \end{bmatrix} + \begin{bmatrix} 0 \\ p n_1 \\ p n_2 \\ p n_3 \\ 0 \end{bmatrix}, \tag{2}$$

$$F^V = \begin{bmatrix} 0 \\ t_{i1} + \tau_{i1} \\ t_{i2} + \tau_{i2} \\ t_{i3} + \tau_{i3} \\ (t_{ij} + \tau_{ij})u_j - q_i - q_i^t \end{bmatrix} n_i, \tag{3}$$

where V is control volume, n_i outer unit normal vector components on its surface, t time, ρ density, u_i velocity vector components, E total energy per unit volume, $H = E + p/\rho$ is total enthalpy and p static pressure. The normal velocity $u_c = u_i n_i$. Summation convention is used for repeated indices. Equation of state for perfect gas is prescribed in the form

$$E = \frac{1}{\gamma - 1}\frac{p}{\rho} + \frac{1}{2}(u_1^2 + u_2^2 + u_3^2) + k, \tag{4}$$

with the ratio of specific heats $\gamma = 1.4$ and k being turbulent energy. The molecular stress tensor and heat flux vector respectively are assumed in the form

$$t_{ij} = \mu 2S_{ij}, \quad S_{ij} = \frac{1}{2}\left(\frac{\partial u_i}{\partial x_j} + \frac{\partial u_j}{\partial x_i}\right) - \frac{2}{3}\delta_{ij}\frac{\partial u_k}{\partial x_k}, \tag{5}$$

$$q_i = -\frac{\gamma}{\gamma - 1}\frac{\mu}{Pr}\frac{\partial(p/\rho)}{\partial x_i}, \tag{6}$$

where δ_{ij} is the Kronecker delta. The dynamic viscosity μ and Prandtl number satisfy

$$\mu = const, \quad Pr = const. \tag{7}$$

The effect of turbulent fluctuations is present by the Reynolds stress tensor τ_{ij} and turbulent heat flux q_i^t, which need to be modeled. An eddy viscosity model assumes

$$\tau_{ij} = \mu_t 2S_{ij} - \frac{2}{3}\delta_{ij}\rho k, \tag{8}$$

$$q_i^t = q_i\frac{Pr}{\mu}\frac{\mu_t}{Pr_t}, \tag{9}$$

where μ_t is eddy viscosity and the turbulent Prandtl number is set $Pr_t = 0.91$. In a k-ω model, the eddy viscosity $\mu_t \sim \rho k/\omega$. The k-ω system can be written

$$\int_V \frac{\partial}{\partial t}\begin{bmatrix} \rho k \\ \rho \omega \end{bmatrix}d\mathcal{V} + \oint_{\partial V} u_c \begin{bmatrix} \rho k \\ \rho \omega \end{bmatrix}d\mathcal{S} = \oint_{\partial V}\begin{bmatrix} (\mu + \sigma_k\mu_t)\frac{\partial k}{\partial x_i} \\ (\mu + \sigma_\omega\mu_t)\frac{\partial \omega}{\partial x_i} \end{bmatrix}n_i dS +$$

$$+ \int_V \begin{bmatrix} P_k - \beta^*\rho\omega k \\ \alpha\frac{\omega}{k}P_k - \beta\rho\omega^2 + CD \end{bmatrix}d\mathcal{V}, \tag{10}$$

where the turbulent production $P_k = \tau_{ij}\frac{\partial u_i}{\partial x_j}$, the α, β, β^*, σ_k, σ_ω are model coefficients and CD a cross-diffusion term, $CD \sim (\partial k/\partial x_i)(\partial\omega/\partial x_i)$. In this work the SST variant of k-ω model is use, see Menter [11].

To take most advantage of the k-ω solution, an explicit algebraic Reynolds stress model (EARSM) can be used having advantage especially in 3D. In the EARSM model proposed by Wallin [12], the Reynolds stress is given by

$$\tau_{ij} = a_{ij}\rho k + \frac{2}{3}\rho k\delta_{ij}, \tag{11}$$

$$\begin{aligned}
a_{ij} = {} & \beta_1 \tau S_{ij} \\
& + \beta_3 \tau^2 (\Omega_{ik}\Omega_{kj} - II_\Omega\delta_{ij}/3) \\
& + \beta_4 \tau^2 (S_{ik}\Omega_{kj} - \Omega_{ik}S_{kj}) \\
& + \beta_6 \tau^3 (S_{ik}\Omega_{kl}\Omega_{lj} + \Omega_{ik}\Omega_{kl}S_{lj} - 2IV\delta_{ij}/3) \\
& + \beta_9 \tau^4 (\Omega_{ik}S_{kl}\Omega_{lm}\Omega_{mj} - \Omega_{ik}\Omega_{kl}S_{lm}\Omega_{mj}),
\end{aligned}$$

where $\tau \sim 1/\omega$ is turbulent time scale, $\Omega_{ij} = \frac{1}{2}\left(\frac{\partial u_i}{\partial x_j} - \frac{\partial u_j}{\partial x_i}\right)$ rotation rate tensor and II_Ω, IV are invariants formed from S_{ij}, Ω_{ij}. The coefficients β_j are taken from Hellsten [2] where also the k-ω system is used for turbulent scales prediction.

In order to model bypass transition to turbulence, the two-equation model of Lodefier and Dick [7] is used. The eddy viscosity is multiplied by turbulence weighting factor

$$\gamma_T = \max[\min(\gamma + \zeta, 1), 0], \tag{12}$$

where γ is near-wall intermittency and ζ free-stream intermittency. The governing equations are

$$\frac{\partial\rho\gamma}{\partial t} + \frac{\partial\rho u_i\gamma}{\partial x_i} = \frac{\partial}{\partial x_i}\left[(\mu + \sigma_\gamma\mu_t)\frac{\partial\gamma}{\partial x_i}\right] + 2\beta_\gamma(1-\gamma)\sqrt{-\ln(1-\gamma)}\rho U_\gamma F_s, \tag{13}$$

$$\frac{\partial\rho\zeta}{\partial t} + \frac{\partial\rho u_i\zeta}{\partial x_i} = \frac{\partial}{\partial x_i}\left[(\mu + \sigma_\zeta\mu_\zeta)\frac{\partial\zeta}{\partial x_i}\right] - C_2\mu_\zeta\frac{U}{U_e^2}\frac{\partial U}{\partial n}\frac{\partial\zeta}{\partial n}, \tag{14}$$

with boundary conditions in the inlet: $\gamma = 0$, $\zeta = 1$, in the outlet: $\partial\gamma/\partial n = \partial\zeta/\partial n = 0$ and on the wall: $\partial\gamma/\partial n = 0$, $\zeta = 0$.

The ζ is zero in the boundary layer. The γ is first zero everywhere and starts to increase to 1 in the turbulent boundary layer as soon as the starting function F_s is activated. In laminar part $F_s = 0$. When a transition criterion is satisfied, the $F_s = 1$. Currently Mayle and Abu-Ghannam, Shaw criteria are used, see [5, 9]. They depend on free stream turbulence level, boundary layer thickness and pressure gradient. The transition on the separation bubble (at shock wave) is not considered. The intermittency γ_T multiplies the turbulent stress and also scales the production

term in k-equation according to:

$$F_G P_k - \min[1.0, \max(\gamma_T, 0.1)]\beta^* \rho \omega k, \tag{15}$$

$$F_G = B + (1. - B)\gamma_T^{0.75}, \ B = 0.056 Tu, \tag{16}$$

where Tu is local turbulence intensity, $Tu = 100\sqrt{2k/3}/U$, where U is magnitude of local velocity.

Solving the above systems of equations, the domain contains 1 period of turbine cascade. Subsonic flow in normal direction is assumed in the inlet as well as in the outlet. Then we prescribe in the inlet: flow angle, total density and total pressure. In the outlet, the mean value of static pressure is fixed which determines the flow regime.

2.2 Numerical Solution

For spatial discretization we use a cell centered finite volume method with quadrilateral (in 2D) or hexahedral (in 3D) finite volumes composing a structured grid. The numerical inviscid flux is computed by the AUSMPW+ splitting [4]. The higher order of accuracy is achieved by linear interpolation in the direction of grid lines with e.g. van Leer limiter. The discretization of diffusive flux is central. The approximation of cell face derivatives needed in diffusive terms uses octahedral dual finite volumes constructed over each face of primary volume – the vertices are located in vertices of primary face and in centers of adjacent primary volumes. For time discretization, the implicit backward Euler scheme is employed where the steady residual at new time level is approximated by linear extrapolation. The Jacobi matrices of the flux are obtained as derivatives of discrete expressions for flux with respect to nodal values from the stencil of implicit operator. We chose 7-point stencil, which leads to block 7-diagonal system of linear equations (not considering boundary conditions). The size of a block equals to the number of coupled equations. Numerical solutions of some 3D cases of incompressible flow are given in [8].

2.3 Remarks to the Implementation of Transition Model

The transition model source terms depend on laminar or turbulent state of boundary layer. Therefore the distinction is needed if the finite volume is inside boundary layer and then if a transition criterion is met. The edge of boundary layer is indicated by magnitude of vorticity vector small enough. The threshold is 1 % of its maximum on normal to the wall, where maximum in attached boundary layer is on the wall. This distance is then further increased by 30 %.

In 3D, only corners with meeting 2 walls are considered (which is the case of present simulation). Then the evaluation of source terms proceeds in grid planes perpendicular to the walls. Each finite volume is assigned either to boundary layer or free stream. Near the corner, however, the magnitude of vorticity is close to zero. Therefore the boundary layer edge is found as intersection point of extrapolation of the 2 still well defined boundaries layers. All points in the corner area are then assigned the free-stream parameters and boundary layer thickness from this intersection.

For parallel implementation it is desirable that the model be local. This is not satisfied when free-stream values or boundary layer thickness are parameters of the model. However the present work uses multi-block grids where it is natural to distribute the work block-wise. Then if the whole thickness of the boundary layer is contained within one block, the evaluation is block-local. This requirement often can be easily satisfied.

3   Computational Results

The 2D simulation is first shown on the tip profile cascade with outlet Mach number $M_{2is} = 1.425$. The tip cascades exhibit low setting angle which brings some features of flow-field typical for isolated profile e.g. closed supersonic region on the suction side. The intermittency γ used with SST turbulence model is shown in Fig. 1. The transition on the upper side occurs earlier than on the lower side, as can be seen also on the wall shear stress in Fig. 2, where negative values of τ_w correspond to upper side (not recirculation). The influence of transition on Mach number is marginal, see Fig. 3. The influence of transition on kinetic energy loss is also small: the loss coefficient is 6.14 % in fully turbulent simulation and 5.90 % in simulation with transition.
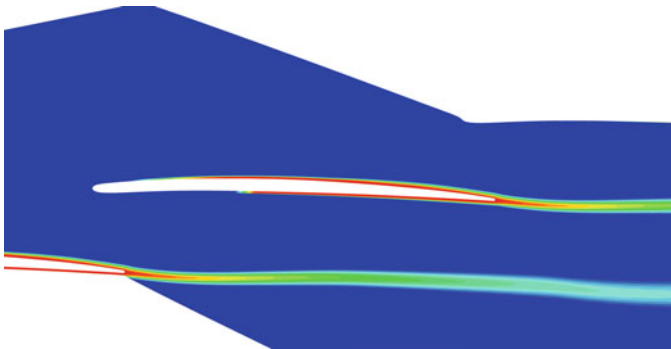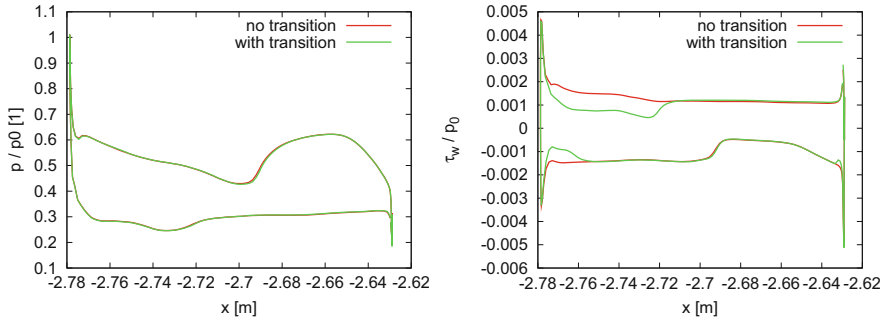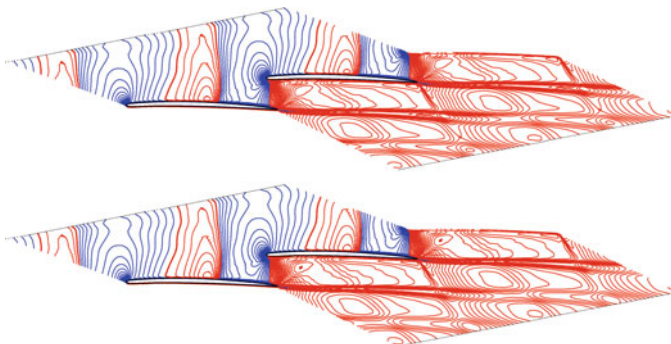

Fig. 1 Tip profile cascade, isolines of intermittency γ

Fig. 2 Tip profile cascade, static pressure and shear stress on the blade surface, influence of transition


Fig. 3 Tip profile cascade, isolines of Mach number (*red* – supersonic, *blue* – subsonic). Above: no transition, below: with model of transition

The 3D transitional flow is shown on well known geometry of the SE1050 turbine cascade with prismatic extension into third dimension. The span is equal to chord length (100 mm) and walls are considered on the sides. The isentropic outlet Mach number is 1.012 and the Reynolds number from chord length $1.2 \cdot 10^6$. The grid has $1.36 \cdot 10^6$ finite volumes with 152 steps in span-wise direction. The grid is refined near walls with minimum wall normal thickness approx. 0.0007 mm. The time step is 10^{-6} s. The EARSM model has been used together with the model of transition. The Fig. 4 shows intermittency γ near the surface (in first layer of finite volumes). It shows that the transition starts on the side walls and near the corners on the suction side of the blade. The pressure side (not shown) is laminar. The flow in mid-plane only starts the transition to turbulence in front of trailing edge but does not reach fully turbulent state there (red color). The influence of transition on the Mach number near the surface is shown in Fig. 5.
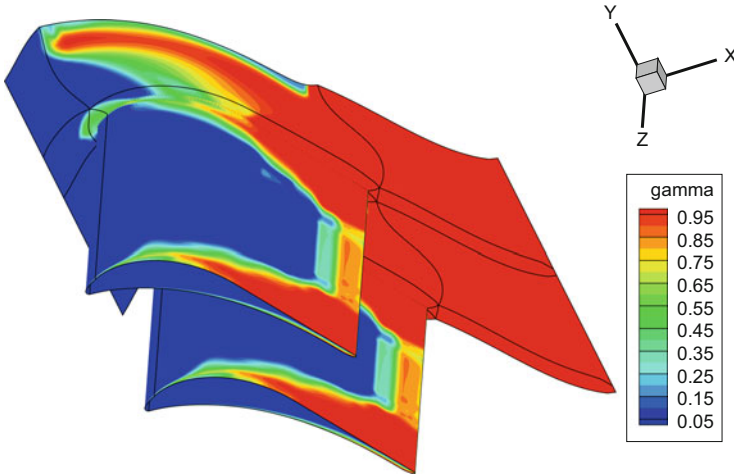
Fig. 4 3D SE1050 cascade, intermittency γ near the walls
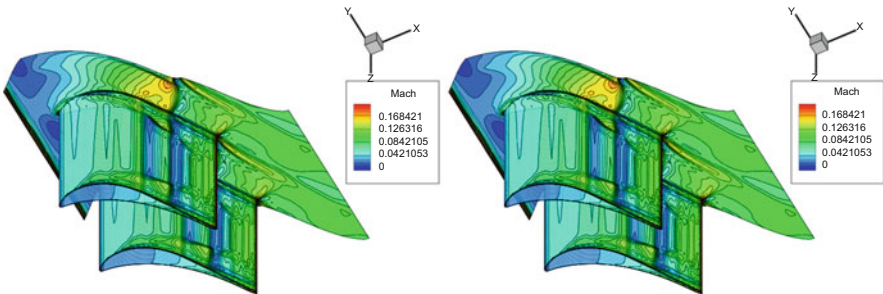
Fig. 5 3D SE1050 cascade, Mach number near the surface. *Left*: fully turbulent, *right*: with transition

The transition on the SE1050 in the mentioned regime occurs late and only on the suction side also for infinite span (i.e. 2D case), as shown in Fig. 6. The influence of transition is visible on the surface shear stress shown in Fig. 7. One can see that the pressure side boundary layer again is practically laminar. The influence of transition on the Mach number isolines is minimal, see Fig. 8. The influence of transition on kinetic energy loss is consequently also small: 5.57 % in fully turbulent simulation and 5.45 % in simulation with transition.
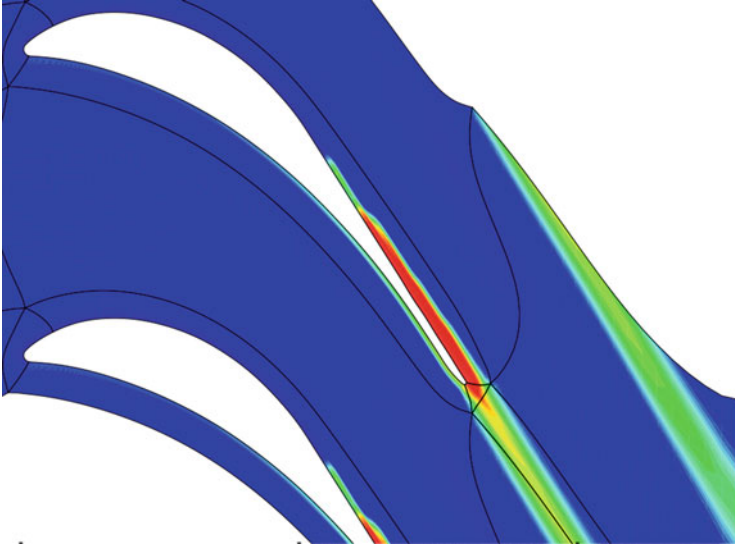
Fig. 6 2D SE1050 cascade, isolines of intermittency γ
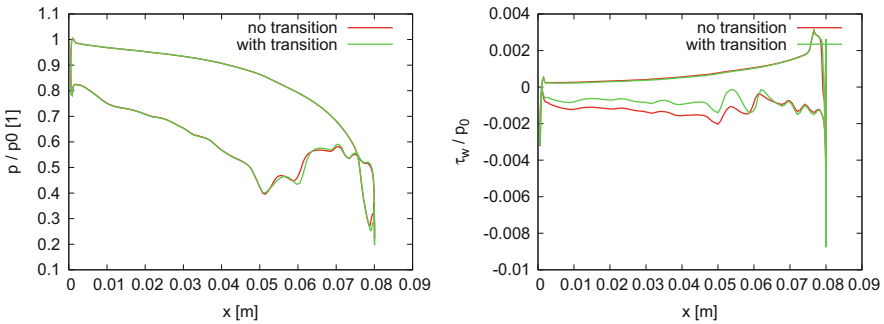

Fig. 7 2D SE1050 cascade, static pressure and shear stress on the blade surface, influence of transition

4 Conclusions

The work presented simulations of 2D and 3D turbulent flow through turbine cascades with eddy-viscosity and EARSM turbulence models complemented with the γ-ζ model of transition to turbulence. The mathematical model is solved by implicit AUSM finite volume method on multi-block structured grids. The implementation of transition model does not rely on explicit prescription of boundary layer edge and is adaptive as long as the whole thickness of boundary layer is contained in one block, which is typically O-grid around the blade (consisting of several blocks in tangential direction). Also the treatment of corners is automatic. The physical
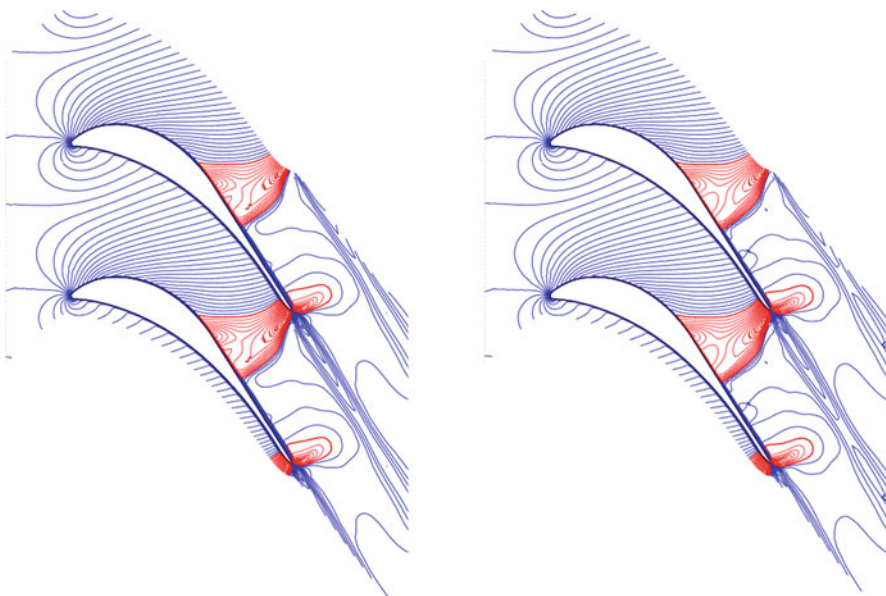
Fig. 8 2D SE1050 cascade, isolines of Mach number (*red* – supersonic, *blue* – subsonic). *Left*: no transition, *right*: with transition

correctness of transition prediction in the flow in convex corner however still needs to be confirmed by measurement. The results are shown for 2D tip profile cascade with very small setting angle and for more classical SE1050 cascade in 2D and 3D. The results exhibit qualitatively correct behavior but quantitatively need to be confirmed by a detailed measurement.

References

1. Durbin, P.: An intermittency model for bypass transition. Int. J. Heat Fluid Flow **36**, 1–6 (2012)
2. Hellsten, A.: New advanced *k-ω* turbulence model for high-lift aerodynamics. AIAA J. **43**, 1857–1869 (2005)
3. Kato, M., Launder, B.E.: The modelling of turbulent flow around stationary and vibrating square cylinders. In: Ninth Symposium on Turbulent Shear Flows, Kyoto (1993)
4. Kim, K.H., Kim, C., Rho, O.-H.: Methods for accurate computations of hypersonic flows I. AUSMPW+ scheme. J. Comput. Phys. **174**, 38–80 (2001)
5. Kubacki, S., Lodefier, K., Zarzycki, R., Elsner, W., Dick, E.: Further development of a dynamic intermittency model for wake-induced transition. Flow Turbul. Combust. **83**, 539–568 (2009)
6. Langtry, R.B., Menter, F.R.: Correlation-based transition modeling for unstructured parallelized computational fluid dynamics codes. AIAA J. **47**, 2894–2906 (2009)

7. Lodefier, K., Dick, E.: Modelling of unsteady transition in low-pressure turbine blade flows with two dynamic intermittency equations. Flow Turbul. Combust. **76**, 103–132 (2006)
8. Louda, P.: Numerical solution of 2D and 3D turbulent inpinging jet flow. Ph.D. thesis, FME CTU, Prague (2002)
9. Mayle, R.E.: The role of laminar-turbulent transition in gas turbine engines. J. Turbomach. **113**, 509–537 (1991). Trans. ASME
10. Medic, G., Durbin, P.A.: Toward improved prediction of heat transfer on turbine blades. J. Turbomach. **124**, 187–192 (2002)
11. Menter, F.R.: Two-equation eddy-viscosity turbulence models for engineering applications. AIAA J. **32(8)**, 1598–1605 (1994)
12. Wallin, S.: Engineering turbulence modeling for CFD with a focus on explicit algebraic Reynolds stress models. Ph.D. thesis, Royal Institute of Technology, Stockholm (2000)
13. Wallin, S., Johansson, A.V.: An explicit algebraic Reynolds stress model for incompressible and compressible turbulent flows. J. Fluid Mech. **403**, 89–132 (2000)
14. Walters, D.K., Cokljat, D.: A three-equation eddy-viscosity model for Reynolds-averaged Navier-Stokes simulations of transitional flow. J. Fluids Eng. **130**, 121401–1–121401–14 (2008)
15. Wilcox, D.C.: Turbulence modeling for CFD. 2nd edn. DCW Industries, Inc. (1998)